VISION BASED CONTROL OF AUTONOMOUS QUADCOPTER FOR TARGET TRACKING

BY

OMAR AWADH AHMED BNHAMDOON

A thesis submitted in fulfilment of the requirement for the degree of Master of Science
(Mechatronics Engineering)

Kulliyyah of Engineering
International Islamic University Malaysia

JANUARY 2021

ABSTRACT

Conventional identification techniques for commercial quadcopters pose several shortcomings, such as limited system order, lack of statistical and non-parametric analysis, and not estimating the model's linear operating range and quadcopter noise dynamics. This affects the prediction accuracy of quadcopter longitudinal and lateral motion dynamics that ultimately limits the quadcopter stabilization. To handle these challenges, in this thesis, statistically suitable plant and noise models are proposed for longitudinal and lateral motion dynamics of AR.Drone 2.0 quadcopter via the Box-Jenkins (BJ) model structure. Utilizing the flight data from the quadcopter, the models were estimated using Prediction Error Method (PEM) guided by statistical, non-parametric, and cross-validation analysis. The goodness of fit showed that the predicted model output matches the measured flight data by 94.72% in the one-step-ahead prediction test. When compared with first and second order models, the results revealed an improvement in prediction accuracy by 52.80%. In terms of image-based control of quadcopter translational dynamics, the rotation sensitivity of normalized spherical image features generates image feature errors and nonlinear coupling effects on the translational degrees of freedom. This causes unsuitable or unnecessary motions, thus affecting the positioning accuracy of the quadcopter. To overcome these limitations, this thesis proposes an image-based position control algorithm using rotation-invariant normalized spherical image features derived from a virtual spherical camera approach and optimally estimated using a Kalman filter method. For longitudinal and lateral translational motion control, the control system comprises an image-based outer-loop control law (developed using a proportional control action) cascaded with a velocity-based inner-loop control law (developed using a discrete-time proportional-integral-derivative (PID) control action). The control of vertical translational motion is based on image-based outer-loop control law. During the combined image-based positioning and hovering tasks, the proposed control algorithm regulates the image feature error in a maximum average time of approximately 25.29 s with a maximum average positioning accuracy of approximately 96.34%. For the combined image-based target tracking and hovering tasks, after the first disturbance of target object has vanished, the proposed control algorithm regulates the image feature error in a maximum average time of approximately 9.06 s. To further enhance the capability of the proposed control system, this thesis proposes an extremum seeking based automatic tuning system to determine the optimal vertical motion servoing gain that will optimize the response of filtered vertical motion image feature. This drastically improved the rise time and the time needed to reach the setpoint by approximately 57.82% and 59.22%, respectively, during image-based positioning tasks. The outcome from this research work had demonstrated adaptive image-based flight controllers which ultimately would be extensively useful for selfie drones, multiple target inspection tasks, and high-speed autonomous drone racing.

Keywords: Quadcopter, PEM method, BJ model, image-based control, spherical image features, image moment features, Kalman filter, extremum seeking.

خلاصة البحث

تواجه طرق التعرف على أنظمة الطائرات رباعية الدفع مجموعة من المشكلات أهمها: محدودية درجة النظام، عدم الخضوع للتحليل الإحصائي و اللاحدودي، و عدم تقدير مدى التشغيل الخطي و ديناميكا إهتزازات و ضوضاء الطائرة. هذه المشكلات تؤثر على دقة التنبؤ بديناميكا الحركة الجانبية و الأمامية الخاصة بالطائرة. هذا يؤدي في النهاية إلى التأثير على إستقرارية و ثبات الطائرة. يسعى هذا البحث إلى معالجة هذه المشكلات من خلال بناء أنظمة مناسبة من الناحية الإحصائية للتنبؤ بديناميكا الحركة الجانبية و الأمامية لطائرة من دون طيار رباعية الدفع إسمها AR.Drone 2.0. سوف يتم بناء هذه الأنظمة من خلال بيانات الطائرة بإستخدام طريقة PEM مدعّمة بطرق التحليل الإحصائي، و اللاحدودي، و التحققي. معيار goodness of fit يظهر قدرة الأنظمة على التنبؤ بإستجابة الطائرة بنسبة 94.72% عند استخدام طريقة one-step-ahead prediction test. أظهرت النتائج أيضا القدرة على تحسين التنبؤ بإستجابة الطائرة بنسبة 52.80% عند مقارنة أداء هذه الأنظمة مع أداء الأنظمة ذو الدرجة الأولى و الثانية. أن حساسية normalized spherical image features للحركة الدورانية الخاصة بالطائرة يسبب أخطاء و إقتران غير خطي على translational degrees of freedom. كل هذه العوامل قد تسبب حركات غير مناسبة أو غير ضرورية تؤثر في النهاية على دقة موضع الطائرة. يسعى هذا البحث لمعالجة هذه التحديات من خلال تطوير خوارزمية تحكم بصرية لحركة الطائرة الخطية بإستخدام normalized spherical image features غير حساسة للحركة الدورانية الخاصة بالطائرة تم فلترتها بإستخدام خوارزمية Kalman filter. نظام التحكم يتكون من خوارزمية تحكم صورية بإستخدام متحكم proportional control و خوارزمية تحكم للسرعة بإستخدام متحكم PID control. النظام المقترح لديه القدرة على تصفير الاخطاء في زمن أقصى قدره 25.29 s مع دقة في موضع الطائرة قيمتها التقريبية 96.34% عند تعقب هدف ثابت. النظام أيضا لديه القدرة على تعقب هدف متحركة مع إمكانية تصفير الاخطاء في زمن أقصى قيمته 9.06 s عند التوقف الاول للهدف. يسعى هذا البحث إلى تحسين أداء خوارزمية التحكم البصرية لحركة الطائرة الخطية من خلال تطوير نظام تعديل ذاتي لقيمة vertical motion servoing gain من أجل الحصول على إستجابة أفضل للحركة العمودية للطائرة من خلال filtered vertical motion image feature. أظهرت النتائج قدرة نظام التعديل المقترح على تحسين حركة الطائرة العمودية عند الوصول إلى هدف ثابت من خلال معياري rise time، time needed to reach the setpoint بنسبة 57.82% و 59.22% على التوالي. أن نتائج هذا البحث العلمي سوف يمكّن من تطوير أنظمة تحكم قابلة للتكيّف مع ديناميكا الطائرة و التي سوف تكون مفيدة جدا لطائرات التصوير الشخصية، لعمليات فحص عدة أهداف ثابتة، و لطائرات السباقات عالية السرعة.

APPROVAL PAGE

I certify that I have supervised and read this study and that in my opinion, it conforms to acceptable standards of scholarly presentation and is fully adequate, in scope and quality, as a thesis for the degree of Master of Science (Mechatronics Engineering)

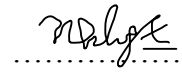

……..
Noor Hazrin Hany Mohamad Hanif
Supervisor

……..
Yasir Mohd Mustafah
Co-Supervisor

I certify that I have read this study and that in my opinion it conforms to acceptable standards of scholarly presentation and is fully adequate, in scope and quality, as a thesis for the degree of Master of Science (Mechatronics Engineering)

……..
Hasmawati Antong
Internal Examiner

……..
Rosmiwati Mohd Mokhtar
External Examiner

This thesis was submitted to the Department of Mechatronics Engineering and is accepted as a fulfilment of the requirement for the degree of Master of Science (Mechatronics Engineering)

……..
Syamsul Bahrin Abdul Hamid
Head, Department of
Mechatronics Engineering

This thesis was submitted to the Kulliyyah of Engineering and is accepted as a fulfilment of the requirement for the degree of Master of Science (Mechatronics Engineering)

……..
Sany Izan Ihsan
Dean, Kulliyyah of Engineering

DECLARATION

I hereby declare that this thesis is the result of my own investigations, except where otherwise stated. I also declare that it has not been previously or concurrently submitted as a whole for any other degrees at IIUM or other institutions.

Omar Awadh Ahmed Bnhamdoon

Signature 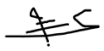 Date 25/09/2020

INTERNATIONAL ISLAMIC UNIVERSITY MALAYSIA

DECLARATION OF COPYRIGHT AND AFFIRMATION OF FAIR USE OF UNPUBLISHED RESEARCH

VISION BASED CONTROL OF AUTONOMOUS QUADCOPTER FOR TARGET TRACKING

I declare that the copyright holders of this thesis are jointly owned by the student and IIUM.

By signing this form, I acknowledged that I have read and understand the IIUM Intellectual Property Right and Commercialization policy.

Affirmed by Omar Awadh Ahmed Bnhamdoon

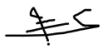

……..……..
Signature

25/09/2020
……..
Date

ACKNOWLEDGEMENTS

Firstly, it is my great pleasure to dedicate this work to my dear mother and my family, who believed in my ability and potential to accomplish this goal: thank you for your continued support.

I would like to express my appreciation and thanks to those who provided their time, advice and guidance for this study. To the members of my dissertation committee, thank you for examining my thesis.

I would like to thank also the Kulliyyah of Engineering and the Office of Postgraduate for giving me the time to finish this research work. This is by extension goes to Mahallah Salahuddin-IIUM for allowing me to use the sport hall during the early stages of this research work.

I would like to express my deepest gratitude and appreciation to my sponsor, *Hadramout Establishment for Human Development (HEHD),* represented by Eng. Abdullah Ahmed Bugshan and all HEHD members for giving me the opportunity to continue my master's degree. Many thanks to you, HEHD, without your support this thesis will not be possible!

Finally, a great thanks to Dr. Noor Hazrin Hany Mohamad Hanif for her continuous help, guidance and leadership, and for that, I will be forever grateful. This is by extension goes to Dr. Yasir Mohd Mustafah for being my co-supervisor during the duration of this research work. Special thanks to Prof. Rini Akmeliawati for her continuous support and assistance in reviewing the publications related to this research work.

TABLE OF CONTENTS

LIST OF TABLES

LIST OF FIGURES

LIST OF SYMBOLS

$\mathbf{e}(\mathbf{t})$	Image feature error vector
$\mathbf{S}(\cdot)$, $\mathbf{S}^*$	Measured and desired image feature error vectors
$\mathbf{d}(\mathbf{t})$	A set of visual data
$\mathbf{m}$	A set of camera and/or target object parameters
u, $\hat{u}$	Optimizing input and optimizing input estimate, respectively
y	System output
$\hat{y}$	Predicted output
$\hat{y}(k\|k-1)$	Model one-step-ahead predicted response
J	Cost function
α_J	Weight factor of cost function
∇J	Gradient of cost function
ρ	Output of high-pass filter
ξ	Output of demodulation process
ω_h	Cutoff frequency of high-pass filter
k	Integrator gain
ω	Frequency of perturbation signal
ϕ	Phase of perturbation signal
a	Amplitude of perturbation signal
$G(z^{-1})$	Plant model
$B(z^{-1})$	Polynomial of order n_b
$F(z^{-1})$	Polynomial of order n_f
$H(z^{-1})$	Noise model
$C(z^{-1})$	Polynomial of order n_c
$D(z^{-1})$	Polynomial of order n_d
n_k	Dead time in samples
n	Zero-mean normally distributed white noise signal
σ_n^2	Variance of white noise signal
ϑ	A set of model coefficients
$\hat{\vartheta}$	Model coefficient estimates

$\varepsilon(k)$	Model residuals
g	Empirical impulse response
h	Empirical step response
$G(\omega)$	Empirical frequency response
γ_{uy}^2	Magnitude-squared coherence
$\Phi_{uu}(\cdot)$	Input spectrum
$\Phi_{yy}(\cdot)$	Output spectrum
$\Phi_{\mathrm{uy}}(\cdot)$	Cross spectrum
$G_\theta(z^{-1})$	Plant model of pitch angle dynamics
$H_\theta(z^{-1})$	Noise model of pitch angle dynamics
$\sigma_{n_{\theta[k]}}^2$	Noise variance of pitch angle dynamics
$F_\theta(z^{-1})$	Polynomial of order n_f of pitch angle dynamics
$G_\phi(z^{-1})$	Plant model of roll angle dynamics
$H_\phi(z^{-1})$	Noise model of roll angle dynamics
$\sigma_{n_{\phi[k]}}^2$	Noise variance of roll angle dynamics
$G_{v_x}(z^{-1})$	Plant model of longitudinal velocity dynamics
$H_{v_x}(z^{-1})$	Noise model of longitudinal velocity dynamics
$\sigma_{n_{v_x[k]}}^2$	Noise variance of longitudinal velocity dynamics
$G_{v_y}(z^{-1})$	Plant model of lateral velocity dynamics
$H_{v_y}(z^{-1})$	Noise model of lateral velocity dynamics
$\sigma_{n_{v_y[k]}}^2$	Noise variance of lateral velocity dynamics
${}^{TF}G_\theta(s)$	Pitch angle comparison model
${}^{TF}G_\phi(s)$	Roll angle comparison model
${}^{TF}G_{v_x}(s)$	Longitudinal velocity comparison model
${}^{TF}G_{v_y}(s)$	Lateral velocity comparison model
$c_1, \cdots, c_{10}$	Coefficients of comparison models
I_{TIC}	Theil's Inequality Coefficient performance metric
I_{fit}	Goodness of fit performance metric
u_θ	Pitch angle command
u_θ^c	Calculated pitch angle command

sat_{u_θ}	Saturation function of pitch angle command
$\underline{u}_\theta$	Minimum allowed pitch angle command
$\overline{u}_\theta$	Maximum allowed pitch angle command
θ	Pitch angle
u_ϕ	Roll angle command
u_ϕ^c	Calculated roll angle command
sat_{u_ϕ}	Saturation function of roll angle command
$\underline{u}_\phi$	Minimum allowed roll angle command
$\overline{u}_\phi$	Maximum allowed roll angle command
ϕ	Roll angle
$u_{\dot{h}}$	Vertical velocity command
ψ	Yaw angle
$K_{p_x}, K_{i_x}, K_{d_x}$	Proportional, integral, and derivative gains of longitudinal motion velocity controller, respectively
$P_x(\cdot), I_x(\cdot), D_x(\cdot)$	Proportional, integral, and derivative terms of longitudinal motion velocity controller, respectively
$K_{p_y}, K_{i_y}, K_{d_y}$	Proportional, integral, and derivative gains of lateral motion velocity controller, respectively
$P_y(\cdot), I_y(\cdot), D_y(\cdot)$	Proportional, integral, and derivative terms of lateral motion velocity controller, respectively
v_{x_b}	Measured longitudinal velocity
$v_{x_b}^*$	Desired longitudinal velocity
$e_{v_{x_b}}(\cdot)$	Error between desired and measured longitudinal velocities
$v_{x_b}^c$	Calculated longitudinal velocity
$sat_{v_{x_b}}$	Saturation function of longitudinal velocity
$\underline{v}_{x_b}$	Minimum allowed value of longitudinal velocity
$\overline{v}_{x_b}$	Maximum allowed value of longitudinal velocity
v_{y_b}	Measured lateral velocity
$v_{y_b}^*$	Desired lateral velocity

$e_{v_{y_b}}(\cdot)$	Error between desired and measured lateral velocities
$v_{y_b}^c$	Calculated lateral velocity
$sat_{v_{y_b}}$	Saturation function of lateral velocity
$\underline{v}_{y_b}$	Minimum allowed value of lateral velocity
$\overline{v}_{y_b}$	Maximum allowed value of lateral velocity
$v_{z_b}^*$	Desired vertical velocity
$v_{z_b}^c$	Calculated vertical velocity
$sat_{v_{z_b}}$	Saturation function of vertical velocity
$\underline{v}_{z_b}$	Minimum allowed value of vertical velocity
$\overline{v}_{z_b}$	Maximum allowed value of vertical velocity
$\mathbf{K}, \mathbf{K}^{-1}$	Camera calibration matrix and its inverse, respectively
$\mathbf{p_d}$	Distorted image point
(u_d, v_d)	Coordinates of distorted image point
$\mathbf{p}$	Undistorted image point
(u, v)	Coordinates of undistorted image point
$\mathbf{p_c}$	Optical center
$(u_0\ , v_0)$	Coordinates of optical center
δ	Distance between distorted point and optical center
$(\rho_w\ , \rho_h)$	Image width and height, respectively
$(\alpha_u\ , \alpha_v)$	Horizontal and vertical scale factors of camera focal length
(r_1, r_2, r_3)	Radial distortion parameters
(t_1, t_2)	Tangential distortion parameters
$\mathcal{F}_W$	World coordinate frame
o_W	Origin of world coordinate frame
x_W, y_W, z_W	Longitudinal, lateral, and vertical axes of world coordinate frame
$\mathcal{F}_B$	Body coordinate frame
o_B	Origin of body coordinate frame
x_B, y_B, z_B	Longitudinal, lateral, and vertical axes of body coordinate frame
$\mathcal{F}_C$	Camera coordinate frame
o_C	Origin of camera coordinate frame

x_C, y_C, z_C	Longitudinal, lateral, and vertical axes of camera coordinate frame
$\mathbf{m_n}$	Normalized image point
(x_n, y_n)	Coordinates of normalized image point
$\mathbf{m_v}$	Virtual image point
(x_v, y_v)	Coordinates of virtual image point
$\alpha_{\mathbf{m_v}}$	Scale factor of virtual image point
$\mathbf{m_s}$	Spherical image point
(x_s, y_s, z_s)	Coordinates of spherical image point
$\alpha_{\mathbf{m_s}}$	Scale factor of spherical image point
(x_c , y_c)	Coordinates of target object center
$\mathbf{R}_\phi$	Rotation matrix depending on roll angle
$\mathbf{R}_\theta$	Rotation matrix depending on pitch angle
$\mathbf{R}_{\phi\theta}$	Rotation matrix depending on roll and pitch angles
${}^{\mathbf{B}}\mathbf{R}_{\mathbf{C}}$, $({}^{\mathbf{B}}\mathbf{R}_{\mathbf{C}})^{-1}$	Rotation matrix between quadcopter body and camera coordinate frames and its inverse, respectively
$sin\,(\cdot)$, $cos\,(\cdot)$	Sine and cosine functions, respectively
$\mathbf{q}$, $\mathbf{q}^*$	Position vector and its desired value, respectively
q_1, q_2, q_3	Longitudinal, lateral, and vertical motion image features, respectively
$q_1^*,\ q_2^*,\ q_3^*$	Desired longitudinal, lateral, and vertical motion image features, respectively
$\tilde{q}_1, \tilde{q}_2, \tilde{q}_3$	Noisy longitudinal, lateral, and vertical motion image features, respectively
$\hat{q}_1,\ \hat{q}_2,\ \hat{q}_3$	Filtered longitudinal, lateral, and vertical motion image features, respectively
$e_{\hat{q}_3}$	Error between desired and filtered vertical motion image features
$(\dot{q}_1, \dot{q}_2, \dot{q}_3)$	Longitudinal, lateral, and vertical motion image feature velocities, respectively
$\mathbf{L_q}$	Feature sensitivity matrix
$\mathbf{m_{s_1}}$, $\mathbf{m_{s_1}}$	First and second spherical image points, respectively
$\alpha_{\mathbf{q}}$	Normalization factor of rotation-invariant normalized spherical image features
$\alpha_{\mathbf{q}_m}$	Normalization factor of normalized image moment features

μ_{pq}	Centred moment of order $p+q$
d_p	Desired depth between quadcopter and target object
r_s	Radius of a virtual sphere formed by two corner target points
$\mathbf{x}$	Image-based state vector
$\mathbf{A}$	State transition matrix
$\mathbf{H}$	Observation matrix
$\widehat{\mathbf{V}}$	Estimated state uncertainty matrix
$\widehat{\mathbf{V}}_{q_1}, \widehat{\mathbf{V}}_{q_2}, \widehat{\mathbf{V}}_{q_3}$	Components of estimated state uncertainty matrix
$\widehat{\mathbf{W}}$	Estimated measurement uncertainty matrix
k	Time instant
T_s	Sampling time
$\mathbf{z}$	Measurement vector
$\lambda_{q_1}, \lambda_{q_2}, \lambda_{q_3}$	Longitudinal, lateral, and vertical motion servoing gains, respectively
$\hat{\lambda}_{q_3}$	Vertical motion servoing gain estimate
T_{end}	End experiment time
T_{rs}	Time needed to reach the setpoint
ϵ	Small positive parameter
ω_h	Frequency parameter of high-pass filter
γ	Adaptation gain
k_{ES}	Iteration index of optimization algorithm
ξ	Mean value of cost function
$\alpha_{\sigma_n^2}$	Design parameter
$\bar{k}_{ES}$	Maximum iterations of optimization algorithm
$M(\cdot), S(\cdot)$	Demodulation and perturbation signals, respectively
$\sim N(0, \sigma^2)$	Follows a zero-mean normal distribution of variance σ^2
t_0 , t_{ES}	Initial and final time instants of image feature error, respectively
$\min(\cdot), \max(\cdot)$	Minimum and maximum functions, respectively
$\mathrm{e}_{\hat{q}_1}, \mathrm{e}_{\hat{q}_2}, \mathrm{e}_{\hat{q}_3}$	Error between desired and filtered longitudinal, lateral, and vertical motion image features, respectively

$e_{\tilde{q}_x}$, $e_{\tilde{q}_y}$, $e_{\tilde{q}_z}$	Error between desired and measured distances along longitudinal, lateral, and vertical axes, respectively
$e_{\tilde{q}_1}$, $e_{\tilde{q}_2}$, $e_{\tilde{q}_3}$	Error between desired and measured longitudinal, lateral, and vertical motion image features, respectively
$\dot{S}_{x_c}, \dot{S}_{y_c}, \dot{S}_{z_c}$	Velocities of longitudinal, lateral, and vertical motion image features for quadcopter camera, respectively
$\mathbf{L}_{\mathbf{S}_v}$, $\mathbf{L}_{\mathbf{S}_\omega}$	Feature sensitivity matrices related to translational and rotational velocities of quadcopter camera, respectively
$v_{x_c}, v_{y_c}, v_{z_c}$	Translational velocities of quadcopter camera along longitudinal, lateral, and vertical axes, respectively
$\omega_{x_c}, \omega_{y_c}, \omega_{z_c}$	Rotational velocities of quadcopter camera along longitudinal, lateral, and vertical axes, respectively

LIST OF ABBREVIATIONS

2-D	Two-dimensional
3-D	Three-dimensional
AP	Actual Position
ACF	Auto Correlation Function
AR	Auto Regressive
BJ	Box Jenkins
CCF	Cross Correlation Function
DOF	Degree of freedom
ES	Extremum Seeking
FIR	Finite Impulse Response
FOV	Field of view
GCS	Ground Control Station
GPS	Global Positioning System
ISE	Integrated Square Error
IMU	Inertial Measurement Unit
ID	Identifier
IBVS	Image Based Visual Servoing
LiPo	Lithium Polymer
MF	Moment Feature
NMES	Neuromuscular Electrical Stimulation
OE	Output Error
OpenCV	Open Source Computer Vision Library
PRBS	Pseudo Random Binary Sequence
PEM	Prediction Error Method
PID	Proportional-Integral-Derivative
PBVS	Position Based Visual Servoing
RGB	Red, Green, Blue
RMSE	Root Mean Square Error
SD	Standard Deviation

SF	Spherical Feature
TF	Transfer Function
UAV	Unmanned Aerial Vehicle
WiFi	Wireless
Q-learning	Quality-learning

CHAPTER ONE
INTRODUCTION

1.1 OVERVIEW

The multirotor Unmanned Aerial Vehicles (UAVs) are aerial machines controlled by changing the speeds of three or more rotating propeller systems. These vehicles have great maneuverability and stable hovering. Nowadays, the development of four-rotor UAVs, known as quadcopters, has gained widespread interests amongst researchers, particularly in terms of dynamic modelling, image-based control, and servoing gain (proportional gain of the image-based control law) tuning. These three components allow to accelerate the deployment of versatile, efficient, and optimal quadcopter technologies in various fields ranging from target tracking missions, aerial photography and videography, to industrial inspection tasks.

For commercial quadcopters, the developed dynamic models are often restricted to first and/or second order models. This affects the prediction ability of the models and leads to inadequate capturing of the quadcopter dynamics. Thus, it is advantageous to have accurate dynamic models for these closed-source vehicles as this will help to understand the dynamics of the "black-box" quadcopter systems at various inputs and control methods. This could be achieved by constructing statistically suitable plant and noise models for the dynamics of longitudinal and lateral motion subsystems of the autopilot system using the Box-Jenkins model structure estimated via prediction error method.

In addition, in image-based control of the quadcopter, the normalized spherical image features utilized in controlling the quadcopter translational dynamics can lead to inadequate quadcopter movements and generate nonlinear coupling between the